The Conjugated Ionospheric Anomalies Preceding the 2011 Tohoku-Oki Earthquake

Liming He[1]*, Lixin Wu[2], Kosuke Heki[3] and Cong Guo[1]

[1]Department of Geodesy and Geomatics, School of Resources and Civil Engineering, Northeastern University, Shenyang, China, [2]School of Geosciences and Info-Physics, Central South University, Changsha, China, [3]Department of Earth and Planetary Sciences, Hokkaido University, Sapporo, Japan

We present the conjugated ionospheric total electron content (TEC) anomalies prior to the 2011 M_w9.0 Tohoku-oki earthquake, Japan, observed by the Global Navigation Satellite System (GNSS) stations in northern Australia. The onset time of the anomaly, determined by the Akaike's information criterion, is 41.5 min before the earthquake in Australia, which is very close to the time observed in Japan. The positive TEC anomalies in Australia emerged on the same longitude as the land area of NE Japan. This supports the model that electric fields within the ionosphere redistributed the electrons immediately before large earthquakes. However, the observed anomaly is shifted equatorward by ~500 km reflecting the difference in physical mechanisms between the two hemispheres. We also found that the geomagnetic declination near the conjugate point simultaneously started to change ~40 min before the earthquake, but its physical implication is yet to be explored.

Keywords: large earthquake, ionospheric anomaly, total electron content, GNSS, conjugate observation

INTRODUCTION

On 11 March 2011, the Tohoku-oki earthquake with a moment magnitude (M_w) 9.0 occurred at the Japan Trench off Northeastern (NE) Japan at 05:46:23 UT. Heki (2011) reported anomalies in ionospheric total electron content (TEC) started ~40 min before the earthquake above NE Japan, using the dense Japanese network of ground Global Navigation Satellite System (GNSS) receivers, GEONET (GNSS Earth Observation Network). Subsequent studies confirmed that similar ionospheric changes were observed immediately before most earthquakes with $M_w \geq 8.2$ where a reasonable number of GNSS stations are available (Heki and Enomoto, 2015). He and Heki (2017) further studied 32 earthquakes with M_w7.0–8.0 in this century and found that the 1/4 earthquakes showed possible preseismic changes starting 20–10 min before earthquakes. Statistical analyses of the 18 earthquakes (M_w7.3–9.2) indicated that leading times, areal extents, and intensities of ionospheric anomalies (relative to background TEC) have a positive correlation with the earthquake magnitude (M_w). A detailed summary of the debates between opponents (Kamogawa and Kakinami, 2013; Utada and Shimizu, 2014; Masci et al., 2015) and our rebuttals (Heki and Enomoto, 2013; 2014; 2015) can be found in the introduction of He and Heki (2017).

He and Heki (2016), He and Heki (2018), and Muafiry and Heki (2020) discussed the three-dimensional (3D) distribution of the positive and negative electron density anomalies responsible for the observed TEC changes. They found that the positive and negative anomalies roughly align along the local geomagnetic field, which suggests that the electric field within the ionosphere may be responsible for the redistribution of the ionospheric electrons (Kuo et al., 2014; Kelley et al., 2017).
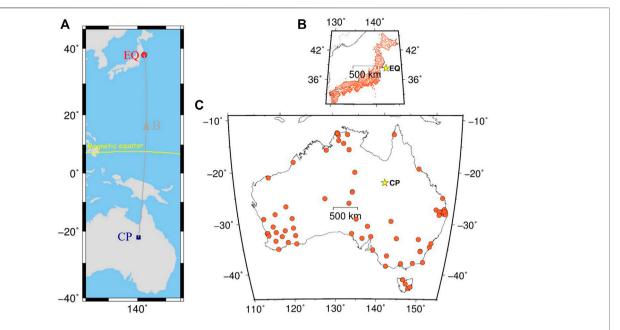
FIGURE 1 | (A) The magnetic conjugate point (CP, blue square) of the epicenter (EQ, red circle) of the 2011 Tohoku-oki earthquake, Japan, lies in northern Australia (the gray curve indicates the ground projection of the geomagnetic field connecting the two points). The yellow curve denotes the magnetic equator. GNSS stations in Japan **(B)** and in Australia **(C)** were drawn using the Hammer equal-area projection. In **(B)** and **(C)**, the red circles represent GNSS stations and the yellow stars show the epicenter **(B)** and its CP **(C)**.

Ionospheric phenomena associated with electric fields within the ionosphere are known to appear simultaneously at two points connected by geomagnetic fields (i.e., conjugated points, CP). Otsuka et al. (2004) and Shiokawa et al. (2005) showed simultaneous emergence of Medium-Scale Traveling Ionospheric Disturbances (MSTID) in Japan and Australia. They also showed that high geomagnetic activities enhance Large-Scale Traveling Ionospheric Disturbances (LSTID) in both hemispheres. However, an individual LSTID within one hemisphere didn't show the synchronously conjugated phenomenon. This supports our understanding that electric fields play important roles in generating MSTIDs, but LSTIDs are excited mechanically as internal gravity waves.

If preseismic ionospheric electron redistributions are due to electric fields, similar ionospheric TEC anomalies would emerge concurrently in the other hemispheres around the CP of the epicenter. We track the location of CP at an altitude of 85 km right over the epicenter of the 2011 Tohoku-oki earthquake using the IGRF-11 model. Here we investigate the behaviors of VTEC around the conjugate region of the epicenter before and after the earthquake occurrence using GNSS stations in Australia.

GNSS DATA AND METHODS

TEC Changes in Australia on 11 March 2011

To investigate the ionospheric TEC variations in Australia associated with the 2011 Tohoku-Oki earthquake, we used raw data from 76 continuously operating GNSS stations in Australia (**Figure 1**). We first converted slant TEC (STEC) to vertical TEC

(VTEC) following He and Heki (2016), by removing the inter-frequency biases of the satellite and receiver, and by multiplying with the cosine of the incident angle of the ray path into a thin shell at 300 km above the ground.

VTEC time series are modeled using polynomial excluding a specific time window possibly influenced by disturbances due to the earthquake. This exclusion window and the polynomial degree should be selected objectively and carefully to isolate the earthquake-related signals. To determine the start of the exclusion window, we followed Heki and Enomoto (2015) to identify the significant bends in VTEC time series before the earthquake using the Akaike's information criterion (AIC). This will be discussed further in *Definition of Reference Curves and Onset Times of the Preseismic Anomaly*. Because we do not have to consider postseismic TEC drops caused by acoustic disturbances associated with coseismic vertical crustal movements (Shinagawa et al., 2013), we fixed the ending time of the excluding window to 20 min after the earthquake.

We utilized the L-curve method to select the optimal polynomial degrees of the reference curves for individual GNSS satellites, following He and Heki (2017). This will be explained in detail in the next section. We define the positive and negative departures from the models as VTEC anomalies. **Figure 2** presents VTEC time series observed using Global Positioning System (GPS) PRN05, 09, and 25 in the southern hemisphere and PRN15 in the northern hemisphere over a 3.5-h interval including the 2011 Tohoku-oki earthquake. Positive anomalies of VTEC (**Figures 2A–1**) start ~40 min before the mainshock around the region to the north of CP in the same way as those observed in Japan (**Figures 2B–1**).
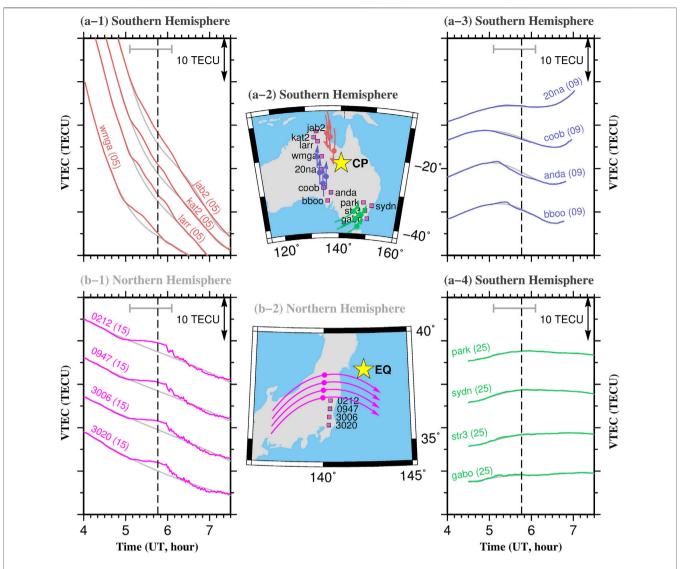
FIGURE 2 | VTEC time series observed using four satellite-station pairs on 11 March 2011 in Australia showing preseismic ionospheric enhancements **(A-1)** around CP, and no significant changes **(A-3, A-4)**. We also show four VTEC time series (b-1) observed in Japan showing preseismic enhancements, which is the VTEC version of **Figure 2** in Heki (2011). The vertical dashed lines show the occurrence of the 2011 Tohoku-oki earthquake. The gray horizontal bars represent the exclusion windows in defining the reference curves. The two maps in the middle panel show the locations of GNSS stations (pink squares) and sub-ionospheric point (SIP) trajectories in Australia **(A-2)** and in Japan **(B-2)**. The circles on the tracks indicate the SIP positions at the earthquake occurrence time. The yellow stars show the epicenter **(B-2)** and it is CP **(A-2)**. We assume the ionospheric height at 350 km to draw the SIP trajectories.

The Japanese data show coseismic ionospheric disturbances ~8 min after the mainshock caused by the acoustic waves excited by the vertical crustal movements (e.g. Astafyeva et al., 2011). Such disturbances are absent in the Australian data. To demonstrate the localized emergence of the anomalies, we show four VTEC time series observed at stations in central Australia (**Figures 2A–3**), and in southeast Australia far from CP (**Figures 2A–4**). Although we set up the same excluding window in defining the reference curves, these TEC time series smoothly connect before and after the earthquake without significant anomalies. Two curves in **Figures 2A–3** (anda, bboo) show an insignificant TEC decrease just before the earthquake, but its relevance to the earthquake is unclear.

Definition of reference curves and onset times of the preseismic anomaly

As He and Heki (2017) discussed, optimal and objective selection of the exclusion window and the polynomial degree is vital to isolate VTEC changes related to earthquakes. VTEC changes with PRN05 have large negative slopes coming from a steep north-south gradient of VTEC (**Figures 2A–1**). We removed constant trends from the curves to make it easier to see the starts of the positive TEC anomalies (**Figure 3**). We show results of the L-curve tests for two of the time series to select the most appropriate degree of polynomials (5 in this case). More examples are shown in **Supplementary Figure S1**.
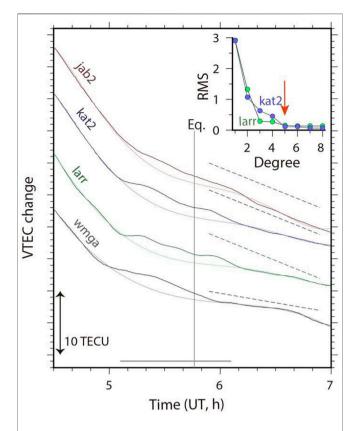
FIGURE 3 | The same VTEC time series as **Figures 2A–1**, but constant trends (attached to each curve as a dashed line) are removed from individual time series for visual clarity of the positive anomalies. The exclusion window is given at the bottom as a horizontal gray line. From the inset showing the behavior of RMS of post-fit residuals (calculated outside the exclusion window) for different polynomial degrees, we considered degree five the most appropriate.

To precisely compare the onset times of ionospheric anomalies in the two hemispheres, we pinpoint the occurrences of the positive breaks in three TEC time series using AIC following Heki and Enomoto (2015). We found significant breaks occurred 42.0 min before the earthquake time in Japan (**Figure 4A**) and 41.5 min before the earthquake time in Australia (**Figure 4B**), respectively. The coincidence suggests that the anomalies started in both hemispheres without significant delays. On the other hand, the amounts of the VTEC rate changes in the two hemispheres were different, i.e. more significant in Australia (**Figure 4C**). We think the difference partly reflects the more considerable background VTEC (~45 TECU) in Australia than in Japan (~30 TECU) (**Figure 4D**).

TEC ANOMALIES AND LSTID

LSTIDs are often observed with GNSS-TEC under active geomagnetic conditions (Tsugawa et al., 2004), making significant bending in TEC time series similar to preseismic anomalies (Heki and Enomoto, 2013). Geomagnetic activity on the day of the 2011 Tohoku-oki earthquake was relatively high, as

shown in the time series of various indices given in **Figure 6A** of Heki and Enomoto (2013). Indeed, Heki and Enomoto (2015) recognized a small amplitude LSTID propagating southward through NE Japan about 1 hour before the earthquake.

We also observed a significant LSTID using GPS PRN05 in southwestern Australia (**Figure 5**). The LSTID emerged above Southwestern Australia around 5.5 UT, ~15 min before the 2011 Tohoku-oki earthquake. It propagated northward with a speed of ~0.6 km/s and reached the north coast of Australia around 6.0 UT. From the difference in time and space, this LSTID is not related to the observations of possible preseismic positive bending in the TEC time series at ~5 UT shown in **Figures 2A–1, A–3**. If these positive TEC anomalies are due to LSTID, we would see signatures like **Figure 5** in **Figures 2A–3** in earlier times. We think this is not the case, and it is unlikely that positive TEC anomalies shown in **Figure 3** are of LSTID origin.

DISCUSSION

Conjugate Effects of Other Large Earthquakes

Seventeen earthquakes of M_w7.3–9.2 with possible preseismic ionospheric TEC anomalies have been reported in addition to the 2011 Tohoku-oki earthquake (Heki and Enomoto, 2015; He and Heki, 2017). To see whether preseismic changes commonly occur around the epicenters of these earthquakes and their CPs, we examined the availability of GNSS data around the CPs of the 17 cases. Unfortunately, we did not find a meaningful amount of GNSS observations (**Figure 6**) near the CPs for 16 earthquakes (they were either within ocean or on land with few GNSS stations). The only exception is Colombia, around the CP of the 2015 Illapel earthquake (M_w8.3). There we observed weak positive TEC enhancements as we reported in He and Heki (2018). However, we considered these results inconclusive because the anomalies were faint.

The TEC anomalies that started together ~40 min before the 2011 Tohoku-oki earthquake in both hemispheres are more significant possibly owing to the larger magnitude (M_w) and higher background VTEC. We also found geomagnetic declination change in Australia (**Supplementary Figure S2**) similar to the change in Japan (Heki and Enomoto, 2013). However, we do not know the physical mechanisms underlying the preseismic geomagnetic field changes. Hence, we do not discuss them in detail in this article.

Spatial Distribution of Conjugate Anomalies

Figure 7 shows the spatial distribution of ionospheric anomalies 1 minute before the earthquake over Australia observed using GPS satellites, PRN02, 05, 09, 12, 25, and 29. Positive anomalies emerged to the north of the CP of the epicenter with a certain westward shift (**Figure 7B**). This also shows that such anomalies do not appear in regions far from the CP despite the same exclusion window used for the analysis. The LSTID shown in **Figure 5** in southwestern Australia around 06:00 UT is outside this map.
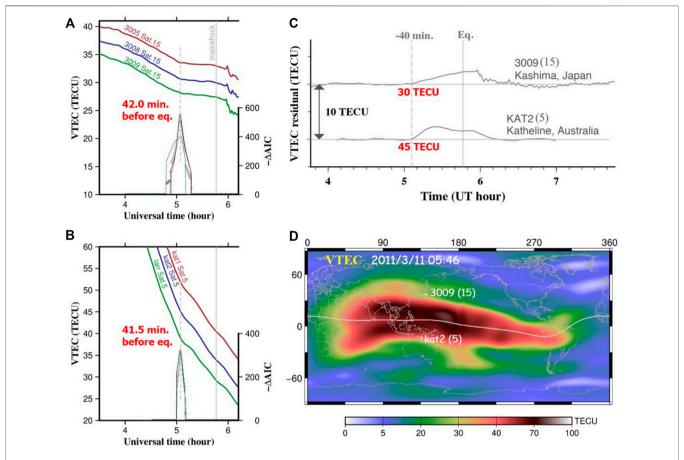
FIGURE 4 | The onset times of the preseismic VTEC enhancements were observed **(A)** near the epicenter of the 2011 M_w9.0 Tohoku-oki earthquake and **(B)** near its CP in Australia, inferred using AIC following Heki and Enomoto (2015). The colored thick curves in **(A)** and **(B)** show the selected VTEC time series before and after the earthquake in Japan and in Australia, respectively (kat1 is very close to kat2). The vertical gray lines represent the earthquake occurrence time. In calculating the–ΔAIC (decrease of AIC by assuming a break at the middle of the moving window), we used the moving time windows of ±30 min, and the absolute and relative thresholds of three TECU/h and 50%, respectively. The time window was shortened to ±20 min for the Australian data. The colored thin curves show the–ΔAIC time series (same colors for same station-satellite pairs). We calculated the averages of the–ΔAIC changes of the three GNSS stations and found significant positive breaks ~40 min before the earthquake both in Japan and Australia. To compare the VTEC rate change, we plot the VTEC residuals from reference curves together with instantaneous VTEC values at the onset time of the anomalies in **(C)** (~30 and ~45 TECU for Japan and Australia, respectively). The global ionospheric map (from ftp.aiub.unibe.ch) in **(D)** shows the VTEC distribution at the earthquake occurrence time. The SIP trajectories same as in **Figure 2** are plotted in **(D)** in white.

For comparison, we also show the spatial distribution of ionospheric anomalies observed using GPS PRN15 in Japan (**Figure 7A**). Due to the limited and sparsely distributed GNSS stations around the CP (**Figure 1C**), it is impossible to reconstruct the 3D structure of the anomalies as He and Heki (2018) did for the 2015 Illapel earthquake. It is also difficult to determine the height of the anomalies by minimizing the scatters of the positive anomalies (He and Heki, 2016) because only one satellite (PRN05) clearly recorded the TEC enhancements.

Implications for Physical Models of Preseismic Ionospheric Anomalies

Two hypotheses have been proposed to explain the observed preseismic ionospheric anomalies. Kuo et al. (2014) showed that the anomaly could be generated by an upward electric current from stressed rock immediately before a large earthquake. This

leads to the westward Hall electric field and the oblique-downward magnetic field drives the downward $E×B$ drift of the ionospheric plasma, and subsequently a pair of positive and negative electron density anomalies. This model, however, needs large electric fields near the ground to let electric current flow overcoming the high atmospheric resistivity there. Kelley et al. (2017) suggested that the $E×B$ drift could be driven directly by surface electric charges. Such charges could produce electric fields in the ionosphere and redistribute ionospheric electrons. A significant difference in this hypothesis is that we require surface electric fields only ~1/500 of the fair-weather field.

We basically support the model by Kelley et al. (2017) but emphasize the importance of induced charges within the ionosphere (**Figure 8**). Electric fields made by surface charges would first penetrate the ionosphere and let electrons redistribute along with geomagnetic fields. If surface charges are positive, the electron will descend and make an electric field opposite to those
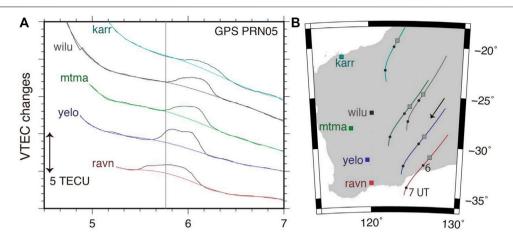
FIGURE 5 | An LSTID was observed using GPS PRN05 in Western Australia propagating northward with a speed of ~0.6 km/s. In **(A)**, we plot the VTEC time series at five stations, shown with squares in **(B)**. The colors of the curves in **(A)** correspond to stations and SIP tracks in **(B)**. Circles on the SIP tracks indicate hourly time marks and grey squares show SIP positions at the time of the earthquake. Reference curves in **(A)** are estimated as polynomials of degree five excluding the time periods influenced by LSTID.

FIGURE 6 | The epicenters (red circles) of eighteen earthquakes ranging from $M_w7.3$ to $M_w9.2$ with possible preseismic ionospheric TEC anomalies and their corresponding conjugate points (blue squares). The white curves show geomagnetic field lines. The yellow curve shows the magnetic equator. The numbers of available GNSS stations are not sufficient when these earthquakes occurred except for the 2011 Tohoku-oki (present study) and the 2015 Illapel (He and Heki, 2018) earthquakes.

made by surface charges. This process would continue until induced electric fields offset the surface-origin electric fields, realizing uniform electric potential within magnetic field lines. The induced charges would result in positive and negative electron density anomalies at the lower and higher ends of magnetic field lines within the ionosphere. This would be the main process that caused positive TEC anomalies just above the surface charges, i.e. above the future epicenter (He and Heki, 2018). This electron redistribution will make an upward electric current, which may be responsible for the eastward temporary magnetic field as observed in NE Japan (Heki and Enomoto, 2013).

Above CP (Australia in **Figure 8**), such induced charges would not develop because of the long distance from the epicenter.

Nevertheless, geomagnetic field lines extending from NE Japan would have electric potential higher than the surrounding field lines, generating electric fields radiating perpendicularly from the magnetic field line. This would make downward/upward *E×B* drift at the western/eastern side of the magnetic field line (**Figure 8**), and positive/negative electron density anomalies in the lower ionosphere (see **Figure 3** of Kuo *et al.* (2011)).

Although the longitudes of the anomalies in both hemispheres are similar, the peak of the positive anomalies in Australia appeared hundreds of kilometers to the north of the epicenter's CP. Downward *E×B* drift would occur at the west side of the geomagnetic field over a large distance along the magnetic field line. This makes a clear contrast to the TEC anomalies in NE Japan where a positive electron density
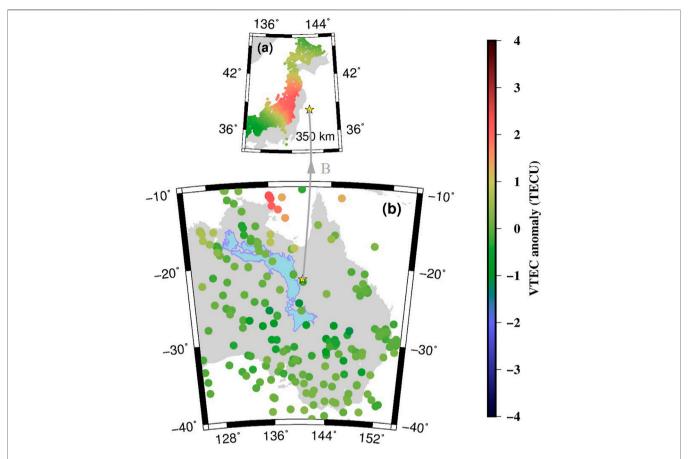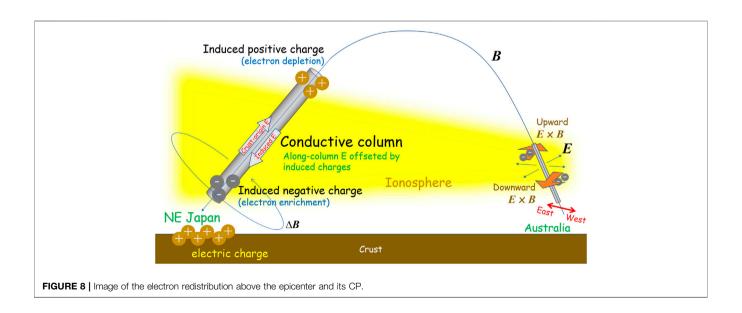
FIGURE 7 | Distribution of VTEC anomalies at 05:45 UT (1 min before the Tohoku-oki earthquake) on 11 March 2011 drawn using GPS PRN02, 05, 09, 12, 25, and 29 in Australia **(B)**, and using PRN15 in Japan **(A)**. The light blue map in **(B)** shows the geomagnetic conjugate image of the Japanese Islands. The yellow stars represent the epicenter of the earthquake in **(A)** and the corresponding CP in **(B)**. The gray curve indicates the ground projection of the geomagnetic field connecting the epicenter and the corresponding CP. We calculated the SIP positions assuming the ionospheric height of 350 km in **(A)** and **(B)**.

FIGURE 8 | Image of the electron redistribution above the epicenter and its CP.

anomaly occurs near the lower end of the geomagnetic field within the ionosphere. Such difference of mechanisms would make different electron density anomalies in the two hemispheres, i.e. they are not exact mirror images as illustrated in Kuo et al. (2011; 2014). This might explain the equatorward shift of the observed positive electron density anomaly above CP.

SUMMARY

In this paper, we observed the geomagnetic conjugate ionospheric TEC anomalies immediately before the 2011 Mw9.0 Tohoku-oki earthquake using the GNSS stations located at Australia in the southern hemisphere. The onset time and magnitude of the ionospheric TEC enhancements in the conjugate region are consistent with the results observed in Japan in the northern hemisphere reported by Heki (2011). For the spatial distribution of the anomalies, the longitudes of the observed TEC enhancements in Australia and in Japan are similar. However, the positive anomalies in Australia appeared ~500 km to the north of the epicenter's CP. The most probable cause for this spatial shift of anomalies is the difference in physical mechanisms between the two hemispheres, i.e., a balanced process between the surface-origin electric fields and the induced electric fields above the future epicenter, which is different from the process in the conjugate region.

A striking feature seen in both hemispheres is that the observed TEC enhancements are stationary, which would be useful to discriminate from other TEC changes, e.g., large-scale traveling ionospheric disturbance, in practical purpose for detection of earthquake-related ionospheric anomalies in the future.

REFERENCES

Astafyeva, E., Lognonné, P., and Rolland, L. (2011). First Ionospheric Images of the Seismic Fault Slip on the Example of the Tohoku-Oki Earthquake. *Geophys. Res. Lett.* 38, a–n. doi:10.1029/2011GL049623

Cahyadi, M. N., and Heki, K. (2015). Coseismic Ionospheric Disturbance of the Large Strike-Slip Earthquakes in North Sumatra in 2012: Mw Dependence of the Disturbance Amplitudes. *Geophys. J. Int.* 200, 116–129. doi:10.1093/gji/ggu343

He, L., and Heki, K. (2017). Ionospheric Anomalies Immediately before M W 7.0-8.0 Earthquakes. *J. Geophys. Res. Space Phys.* 122 (8), 8659–8678. doi:10.1002/2017ja024012

He, L., and Heki, K. (2016). Three-dimensional Distribution of Ionospheric Anomalies Prior to Three Large Earthquakes in Chile. *Geophys. Res. Lett.* 43 (14), 7287–7293. doi:10.1002/2016gl069863

He, L., and Heki, K. (2018). Three-Dimensional Tomography of Ionospheric Anomalies Immediately before the 2015 Illapel Earthquake, Central Chile. *J. Geophys. Res. Space Phys.* 123 (5), 4015–4025. doi:10.1029/2017JA024871

Heki, K., and Enomoto, Y. (2015). M W Dependence of the Preseismic Ionospheric Electron Enhancements. *J. Geophys. Res. Space Phys.* 120, 7006–7020. doi:10.1002/2015ja021353

Heki, K., and Enomoto, Y. (2013). Preseismic Ionospheric Electron Enhancements Revisited. *J. Geophys. Res. Space Phys.* 118 (10), 6618–6626. doi:10.1002/jgra.50578

Heki, K., and Enomoto, Y. (2014). Reply to Comment by K. Heki and Y. Enomoto on "Preseismic Ionospheric Electron Enhancements Revisited". *J. Geophys. Res. Space Phys.* 119 (7), 6016–6018. doi:10.1002/2014ja020223

DATA AVAILABILITY STATEMENT

The original contributions presented in the study are included in the article/**Supplementary Material,** further inquiries can be directed to the corresponding author.

AUTHOR CONTRIBUTIONS

Conceptualization, methodology and original draft preparation, LH; review and editing, LW and KH; visualization, CG.

FUNDING

ACKNOWLEDGMENTS

SUPPLEMENTARY MATERIAL

The Supplementary Material for this article can be found online at: https://www.frontiersin.org/articles/10.3389/feart.2022.850078/full#supplementary-material

Heki, K. (2011). Ionospheric Electron Enhancement Preceding the 2011 Tohoku-Oki Earthquake. *Geophys. Res. Lett.* 38 (17), L17312. doi:10.1029/2011gl047908

Kamogawa, M., and Kakinami, Y. (2013). Is an Ionospheric Electron Enhancement Preceding the 2011 Tohoku-Oki Earthquake a Precursor? *J. Geophys. Res. Space Phys.* 118 (4), 1751–1754. doi:10.1002/jgra.50118

Kelley, M. C., Swartz, W. E., and Heki, K. (2017). Apparent Ionospheric Total Electron Content Variations Prior to Major Earthquakes Due to Electric Fields Created by Tectonic Stresses. *J. Geophys. Res. Space Phys.* 122 (6), 6689–6695. doi:10.1002/2016ja023601

Kuo, C. L., Huba, J. D., Joyce, G., and Lee, L. C. (2011). Ionosphere Plasma Bubbles and Density Variations Induced by Pre-earthquake Rock Currents and Associated Surface Charges. *J. Geophys. Res.* 116, a–n. doi:10.1029/2011JA016628

Kuo, C. L., Lee, L. C., and Huba, J. D. (2014). An Improved Coupling Model for the Lithosphere-Atmosphere-Ionosphere System. *J. Geophys. Res. Space Phys.* 119, 3189–3205. 2013JA019392. doi:10.1002/2013ja019392

Masci, F., Thomas, J. N., Villani, F., Secan, J. A., and Rivera, N. (2015). On the Onset of Ionospheric Precursors 40 Min before Strong Earthquakes. *J. Geophys. Res. Space Phys.* 120 (2), 1383–1393. doi:10.1002/2014ja020822

Muafiry, I. N., and Heki, K. (2020). 3-D Tomography of the Ionospheric Anomalies Immediately before and after the 2011 Tohoku-Oki (M W 9.0) Earthquake. *J. Geophys. Res. Space Phys.* 125 (10), e2020JA027993. doi:10.1029/2020JA027993

Otsuka, Y., Shiokawa, K., Ogawa, T., and Wilkinson, P. (2004). Geomagnetic Conjugate Observations of Medium-Scale Traveling Ionospheric Disturbances

at Midlatitude Using All-Sky Airglow Imagers. *Geophys. Res. Lett.* 31, L15803. doi:10.1029/2004GL020262

Shinagawa, H., Tsugawa, T., Matsumura, M., Iyemori, T., Saito, A., Maruyama, T., et al. (2013). Two-dimensional Simulation of Ionospheric Variations in the Vicinity of the Epicenter of the Tohoku-oki Earthquake on 11 March 2011. *Geophys. Res. Lett.* 40, 5009–5013. doi:10.1002/2013GL057627

Shiokawa, K., Shiokawa, K., Otsuka, Y., Tsugawa, T., Ogawa, T., and Wilkinson, P. (2005). Geomagnetic Conjugate Observation of Nighttime Medium-Scale and Large-Scale Traveling Ionospheric Disturbances: FRONT3 Campaign. *J. Geophys. Res.* 110, A05303. doi:10.1029/2004JA010845

Tsugawa, T., Saito, A., and Otsuka, Y. (2004). A Statistical Study of Large-Scale Traveling Ionospheric Disturbances Using the GPS Network in Japan. *J. Geophys. Res.* 109, A06302. doi:10.1029/2003JA010302

Utada, H., and Shimizu, H. (2014). Comment on "Preseismic Ionospheric Electron Enhancements Revisited" by K. Heki and Y. Enomoto. *J. Geophys. Res. Space Phys.* 119 (7), 6011–6015. doi:10.1002/2014ja020044